

Motion insensitive 3D T2 and T1-weighted imaging with a real-time, image-based PROspective MOtion correction technique (3D PROMO) and automated re-acquisition of motion-corrupted k-space segments

A. Shankaranarayanan¹, E. Han¹, C. Roddey², N. White³, R. Busse⁴, J. Kuperman⁵, J. Santos⁶, D. Rettmann⁷, E. Schmidt⁸, and A. Dale⁹

¹Global Applied Science Lab, GE Healthcare, Menlo Park, CA, United States, ²Dept. of Neurosciences, UCSD, San Diego, CA, United States, ³Dept. of Cognitive Science, UCSD, San Diego, CA, United States, ⁴Global Applied Science Lab, GE Healthcare, Madison, WI, United States, ⁵Dept. of Radiology, UCSD, San Diego, CA, United States, ⁶Dept. of Electrical Engineering, Stanford University, Palo Alto, CA, United States, ⁷Global Applied Science Lab, GE Healthcare, Rochester, Minn, United States, ⁸Global Applied Science Lab, GE Healthcare, Boston, MA, United States, ⁹Dept. of Neurosciences and Radiology, UCSD, San Diego, CA, United States

Introduction

Patient motion during an MRI scan can cause significant artifacts in the acquired images, compromising their diagnostic value. Motion can be especially problematic when imaging “uncooperative” patient populations (e.g. non-anesthetized pediatric, geriatric, or seizure patients) and during long high-resolution 3D scans. To address the confounding nature of motion, a novel real-time image-based 3D PROspective MOtion correction method (3D PROMO) was previously presented [1] and specifically described in the context of motion insensitive 3D T1-weighted imaging (3D T1w PROMO) [2]. To provide a more complete motion correction solution for 3D imaging, this work implements a motion insensitive 3D T2-weighted imaging sequence by integrating 3D PROMO with a 3D FSE acquisition (3D T2w PROMO). In addition, an automated re-acquisition of motion-corrupted k-space views was devised to further increase the robustness of PROMO. Brain images acquired during subject motion demonstrate the feasibility and effectiveness of 3D T2w and T1w PROMO.

Methods

Navigators: Sets of 3 orthogonal low-flip, single-shot spiral acquisitions (S-Nav) were integrated into 3D Fast Spin Echo (FSE) and 3D Inversion-Recovery (IR) SPGR pulse sequences. Images reconstructed from these spiral acquisitions were the primary inputs to the real-time motion estimation algorithm. Spiral parameters: TE/TR=3.4/14 ms, FA=5° (to minimize the impact of signal saturation on the acquired 3D volume), FOV=32 cm, slice thick=15 mm, 2048 points, BW=±125 kHz

3D T2: S-Navs and code for real-time slab re-positioning were integrated into the T1-recovery time of a 3D FSE pulse sequence (3D FSE Cube) without impacting imaging time (Fig 1). 3D FSE Cube with eXtended Echo Train Acquisition (XETA) utilizes variable flip refocusing [3] optimized to be less sensitive to motion and flow [4]. Sequence parameters: TE/TR=100/2000 ms, FOV=20 cm, slice thick=1.3 mm, acquisition matrix=160x160x160, ETL=94, BW=±31.25 kHz.

3D T1: 3D IR-SPGR sequence with 3D PROMO was previously described [2]. S-Navs were inserted into a 3D IR-SPGR sequence prior to each inversion pulse (Fig 1).

Motion estimation: As described in [1, 2], 3D PROMO relies on the Extended Kalman Filter to estimate, for every set of acquired S-Nav images, all 6 rigid-body motion parameters. These motion estimates are then used by the pulse sequence to re-position the imaging volume and the location of subsequent S-Nav planes in real-time. In this work, two new features were added to the previously described method to increase its robustness: (i) Automated re-acquisition (rescan) of motion-corrupted k-space segments (ii) Automatic generation of an S-Nav mask based on S-Nav images acquired at the very beginning of each 3D PROMO sequence. The S-Nav mask segments the brain from the rest of the head in subsequently acquired S-Nav images, allowing the rigid-body motion estimation algorithm to ignore motion in regions of the head that move non-rigidly with respect to the brain (e.g. neck, jaw, orbits).

Rescan: A rescan metric was defined: $\rho = \|m(n)_{t=1} - m(n)_{t=0}\|$ where m is a vector comprised of the 6 rigid body motion estimates [$t_x, t_y, t_z, r_x, r_y, r_z$] in mm and degrees, $t=0$ represents the time of the last S-Nav prior to the acquisition of the n^{th} k-space segment (i.e. n^{th} echo train for 3D FSE Cube and n^{th} IR segment for 3D IR-SPGR) and $t=1$ the time of the first S-Nav subsequent to acquisition of the same n^{th} k-space segment (Fig 1). During image acquisition, ρ was calculated for every acquired k-space segment in real-time. After the entire imaging volume was acquired, all k-space segments with ρ greater than a threshold ($\rho > 1.0$) were re-scanned.

In vivo experiments: Following informed consent, volunteer experiments were performed with 3D T2w PROMO and 3D T1w PROMO on a 1.5T GE Signa HDx scanner (Waukesha, WI). The experiments consisted of 3 scans: (i) a scan without motion correction where the volunteer was asked to perform multiple random motions during the scan, (ii) a 3D PROMO scan where the volunteer approximates the same motions as in (i), and (iii) a baseline “gold-standard” scan where the volunteer was asked to stay as still as possible. Performed motions exercised all 6 rigid body motion parameters.

Results

As shown by representative images in Fig 2, 3D PROMO greatly improves image quality (IQ) in the presence of motion. The IQ obtained during motion (Fig 2.ii.) was qualitatively comparable with the IQ acquired without motion (Fig 2.iii.). As also shown in Fig 2, the inserted S-Nav pulses did not cause noticeable saturation effects in the acquired 3D PROMO images. In the experiments performed, rescans increased scan time by a negligible amount (~5%). Figure 3 shows a representative example of the 6 rigid-body motion estimates calculated during a typical motion experiment.

Discussion and Conclusion

This study demonstrates the effectiveness of 3D PROMO to accurately detect and correct – in real time – rigid body motions that occur during high-resolution 3D FSE Cube and 3D IR-SPGR imaging. Future studies will evaluate the effectiveness of 3D PROMO in clinically relevant “uncooperative” patient populations.

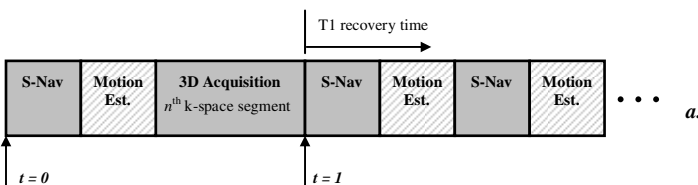


Fig 1: Pulse sequence block diagram. New motion parameters are estimated once every echo train (for 3D FSE) and once every IR segment (for 3D IR-SPGR). Sequence “dead-time” follows every S-Nav acquisition to allow time for calculation of motion estimates. Low-flip S-Nav acquisitions are inserted to fill 3D sequence’s intrinsic T1 recovery time.

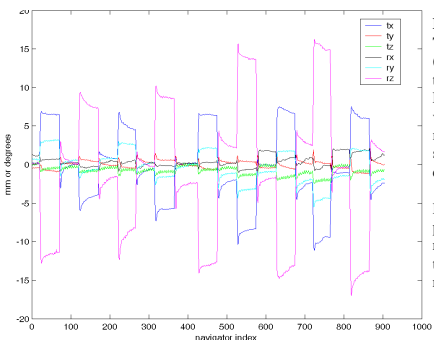


Fig 3: Example of motion estimates. The six rigid-body motion estimates ($t_x, t_y, t_z, r_x, r_y, r_z$) calculated during the acquisition of image shown in Fig 2.ii.d. During the experiment, the volunteer was asked to perform motions during the entire length of the scan. All 6 motion parameters were exercised.

Dominant motion parameters for this particular experiment:
 $r_z = [-15 \ 15]$ degrees
 $t_x = [-12 \ 8]$ mm
 $r_y = [-5 \ 3]$ degrees

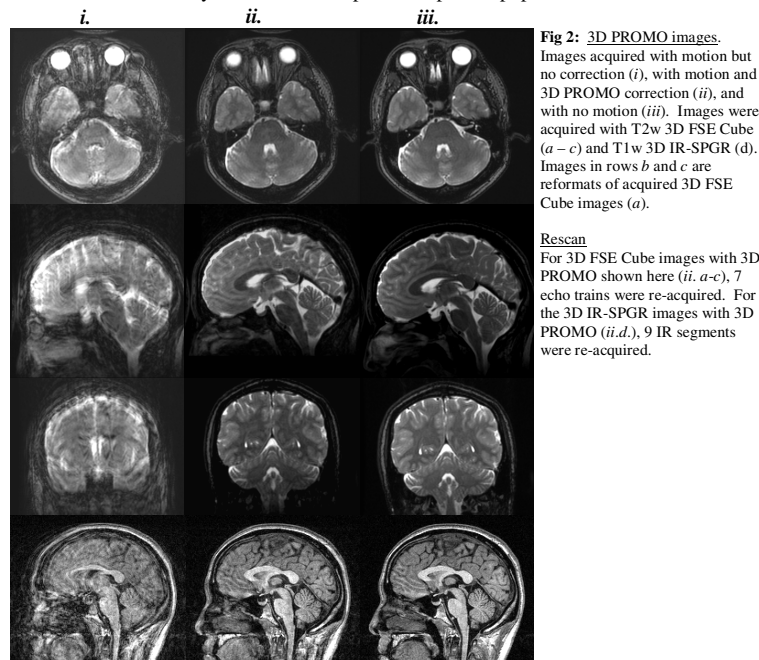


Fig 2: 3D PROMO images. Images acquired with motion but no correction (i), with motion and 3D PROMO correction (ii), and with no motion (iii). Images were acquired with T2w 3D FSE Cube (a - c) and T1w 3D IR-SPGR (d). Images in rows b and c are reformats of acquired 3D FSE Cube images (a).

Rescan
 For 3D FSE Cube images with 3D PROMO shown here (ii. a-c), 7 echo trains were re-acquired. For the 3D IR-SPGR images with 3D PROMO (ii.d.), 9 IR segments were re-acquired.

References: [1] White N et al. ISMRM 2007, p 1829. [2] Shankaranarayanan et al. ISMRM 2007, p 2117. [3] Mugler et al. ISMRM 2000, p 687. [4] Busse et al. ISMRM 2007, p 1702.